# Electronic Supporting Information for:

# Hydroxyl Improving the Activity, Selectivity and Stability of Supported Ni Single Atom for Selective Semi-Hydrogenation

Minzhen Jian,[a] Jin-Xun Liu[a*] and Wei-Xue Li[ab*]

[a] Department of Chemical Physics, School of Chemistry and Materials Science, University of Science and Technology of China, Hefei, Anhui 230026, China

[b] Hefei National Laboratory for Physical Sciences at the Microscale, Hefei, Anhui 230026, China

[*] Electronic mail: wxli70@ustc.edu.cn jxliu86@ustc.edu.cn

Table of Contents

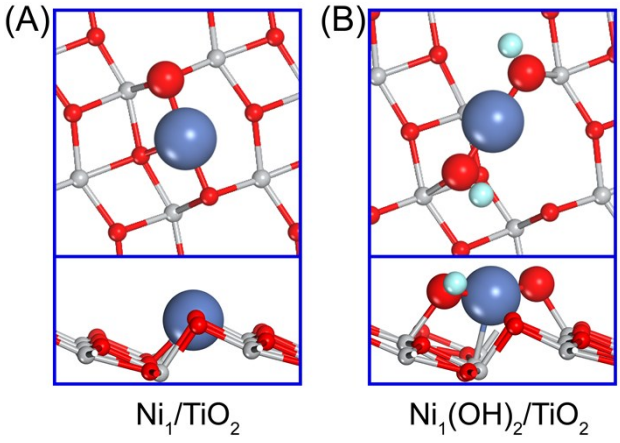


Figure S1. Top view and side view structure of (A) $Ni_1/TiO_2$ and (B) $Ni_1(OH)_2/TiO_2$.

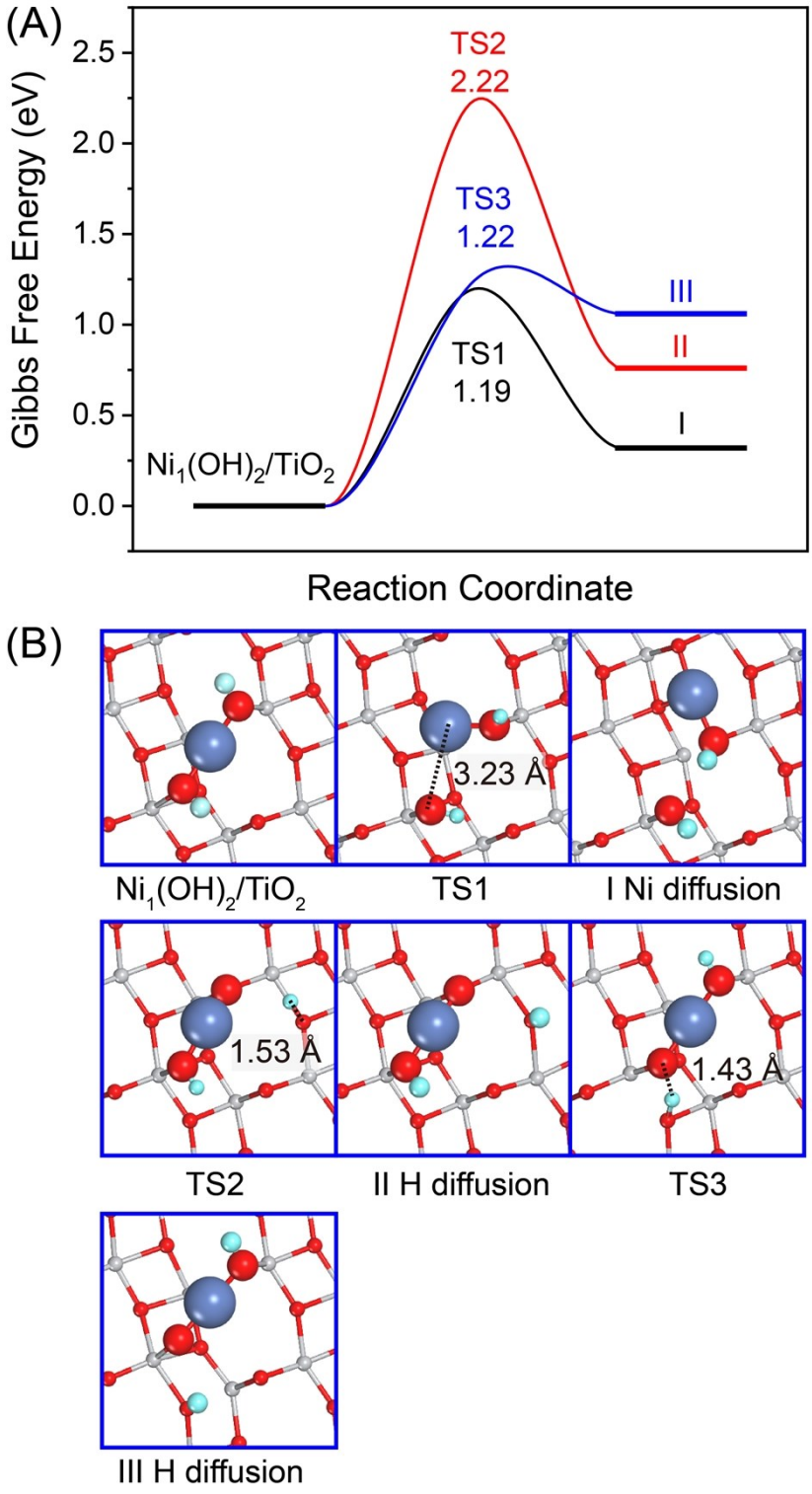


Figure S2. The stability of Ni atom and H in $Ni_1(OH)_2/TiO_2$. (A)The diffusion energy with Gibbs free energy correction of Ni atom and H atom at 360 K, (B) corresponding structures. The black line represents the Ni diffusion to adjacent hollow site, the blue line represents the H in left OH diffusion to adjacent $O_{3c}$ site, the red line represents the H in right OH diffusion to adjacent $O_{3c}$ site.

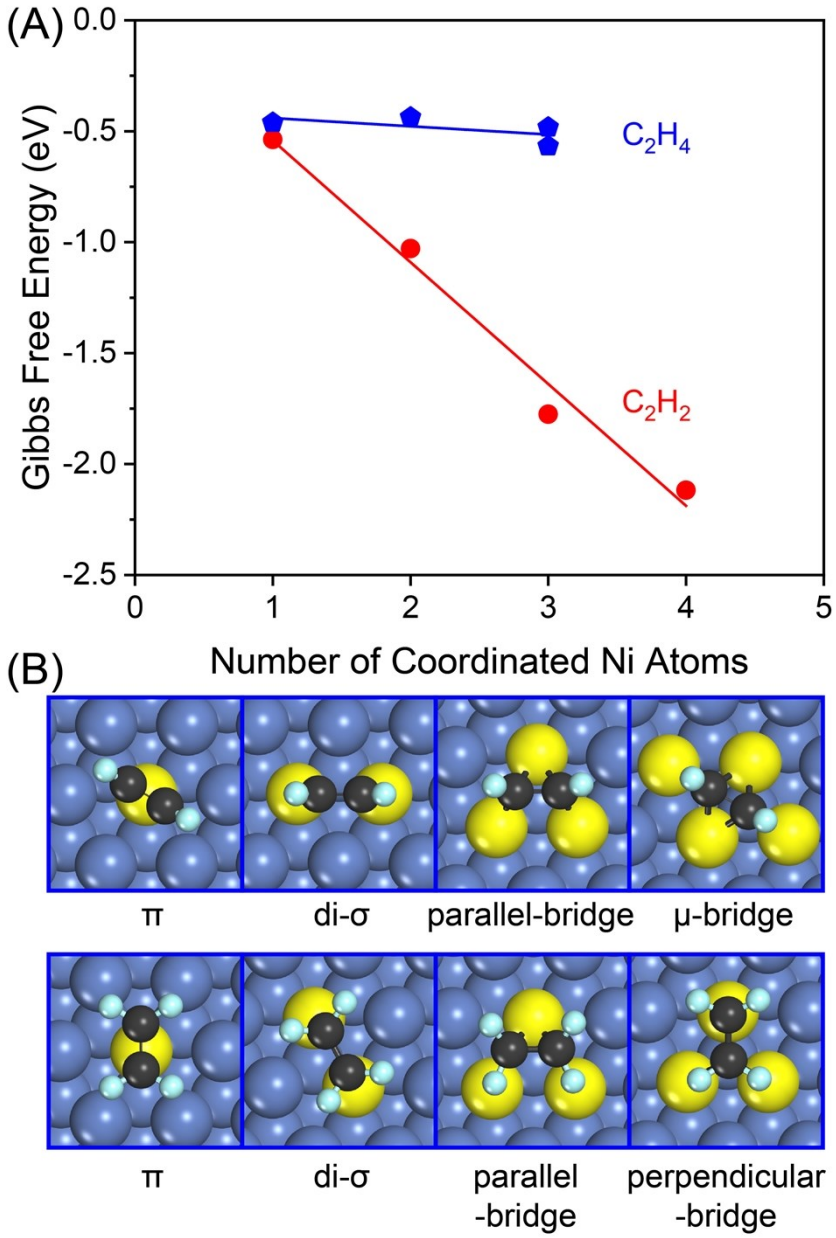


Figure S3. (A) Structure-energy relations between the adsorption energy with Gibbs free energy correction of $C_2H_2$/$C_2H_4$ and the number of coordinated nickel atom at 360 K in total pressure of 0.1MPa, 0.5% $C_2H_2$, 25% $C_2H_4$ and 5% $H_2$, respectively. (B)Top view of the adsorption of $C_2H_2$ (up) and $C_2H_4$ (bottom) on various sites of the Ni (111) surface. The Ni atom coordinated with C atoms were highlighted with yellow ball. Color code: Ni(blue), C(black), H(green).

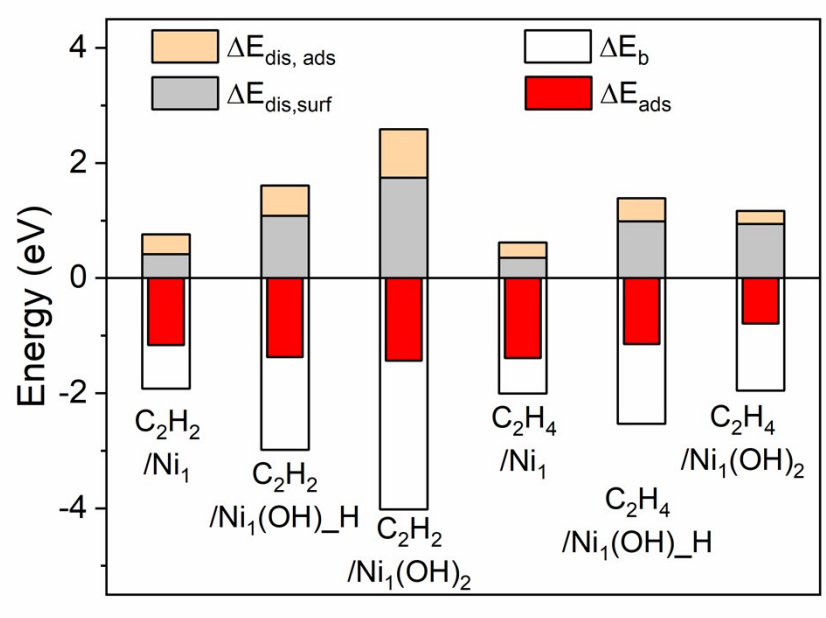


Figure S4. Decomposition of adsorption energies of acetylene and ethylene on different $Ni_1/TiO_2$, $Ni_1(OH)\_H/TiO_2$ and $Ni_1(OH)_2/TiO_2$ single atom catalysts.

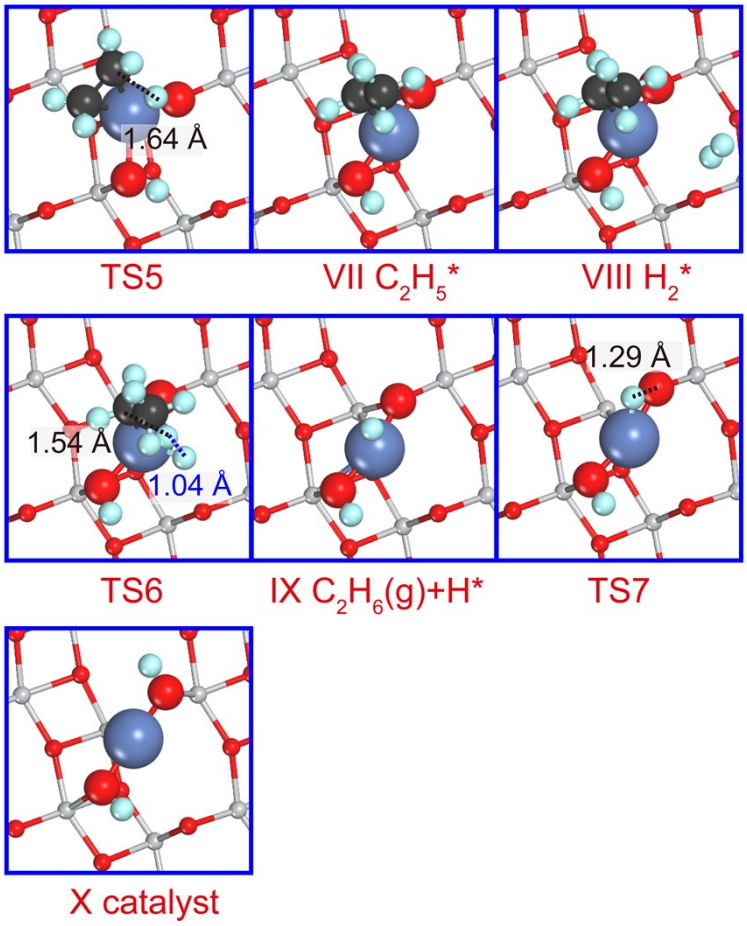


Figure S5. Corresponding structures of sequential hydrogenation of ethylene to ethane over $Ni_1(OH)_2/TiO_2(101)$. Blue, gray, red, black and green balls are nickel, titanium, oxygen, carbon and hydrogen atoms, respectively.

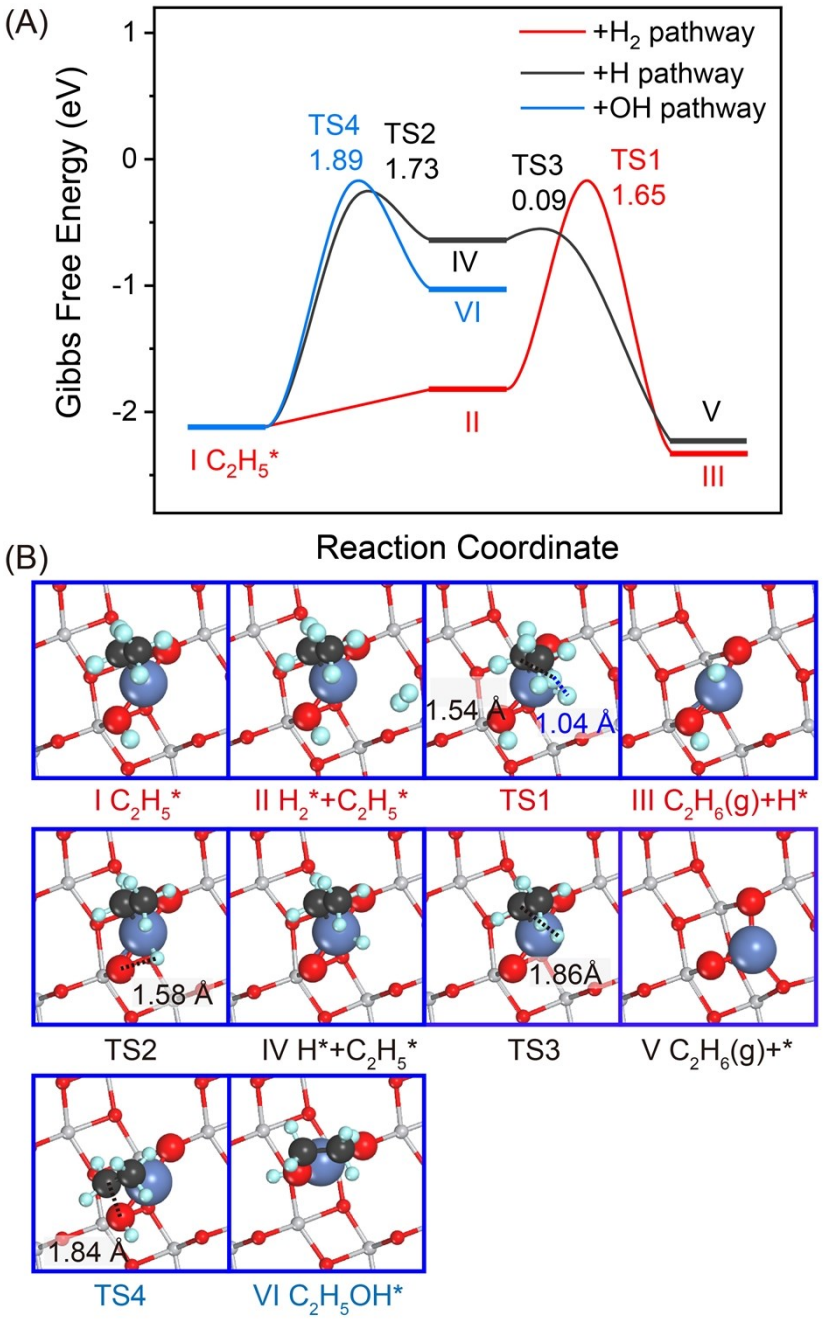


Figure S6. Gibbs free energy diagram and corresponding configurations for the removal of the intermediate ($C_2H_5$*) through hydrogenation by $H_2$ (red line), H in OH (black line) and coupling with OH (blue line). Color code: Ni (blue), C (black), H (green), Ti(gray), O (red).

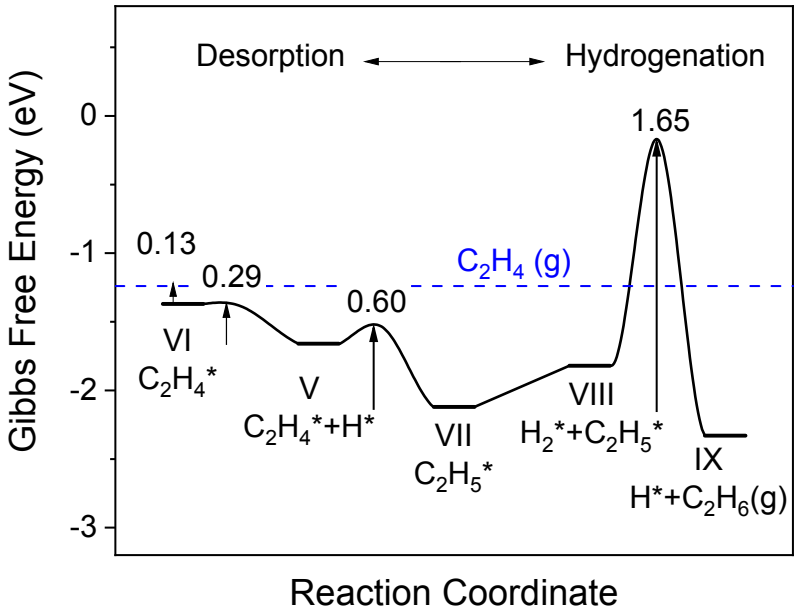


Figure S7. Gibbs free energy diagram of competitive reaction pathway for $C_2H_5$* (VII) hydrogenation and dehydrogenation. Corresponding structures are shown in Figure 3 and Figure S5.

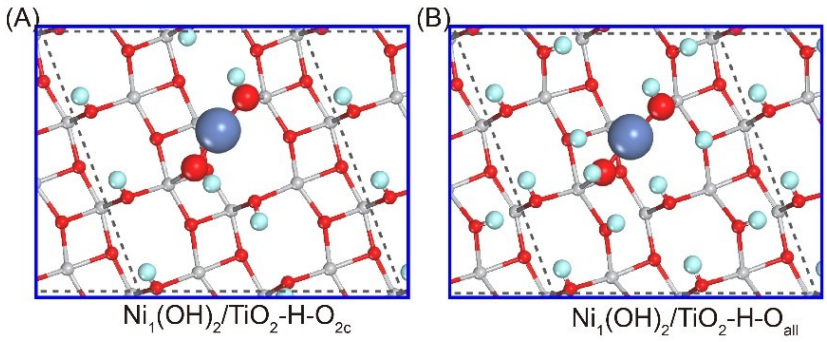


Figure S8. The structures of (A) $Ni_1(OH)_2/TiO_2$-H-$O_{2c}$ and (B) $Ni_1(OH)_2/TiO_2$-H-$O_{all}$, representing H adsorption at two-coordinated O sites and H at all surface O sites, respectively.

For the cases of hydrogenated $Ni_1(OH)_2$/TiO2 surfaces, we systematically evaluated the effect of surface hydrogen on the activity of acetylene hydrogenation at the Ni single atom site. First of all, the surface coverage of H was estimated. H can adsorb at the three-coordinated O site and two-coordinated O site. We found H adsorbs at the two-coordinated O site (Figure S7 A) stable with an exothermic adsorption of -0.13 eV per H atom. However, H at three-coordinated O site is unstable, reflecting from the highly endothermic adsorption energy of H on all surface O site of +0.25 eV per H atom (Figure S7 B). Therefore, H adsorbs at the two-coordinated O site was used as the model catalyst to study the effect of hydrogenations of surfaces on catalytic performance of acetylene hydrogenation.

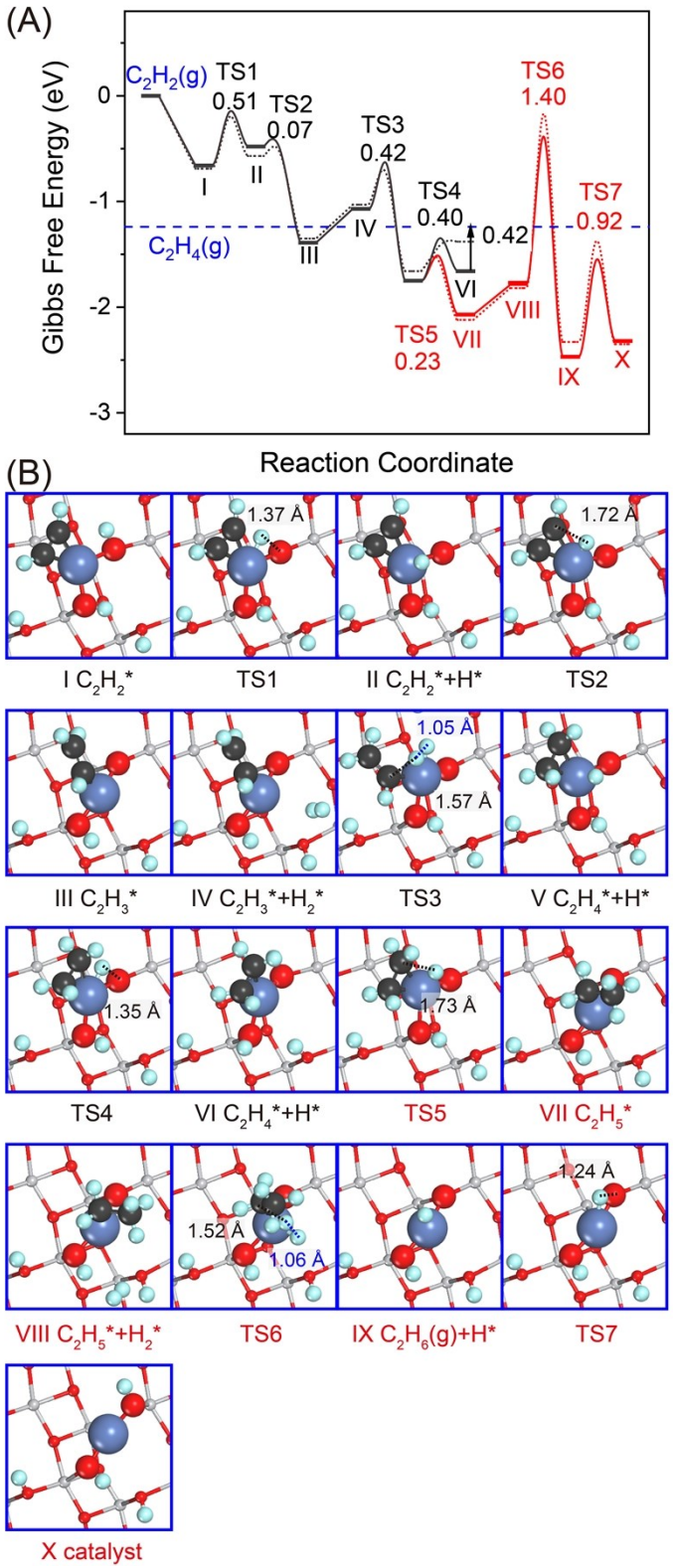


Figure S9. Gibbs free energy diagram (A) and corresponding configurations (B) for acetylene hydrogenation towards ethane on $Ni_1(OH)_2/TiO_2$-H (solid line) and $Ni_1(OH)_2/TiO_2$(dot line) catalyst. The Gibbs free energy was corrected at 360 K in total pressure of 0.1MPa with 0.5% $C_2H_2$, 25% $C_2H_4$ and 5% $H_2$, respectively. Color code: Ni (blue), C (black), H (green), Ti(gray), O (red).

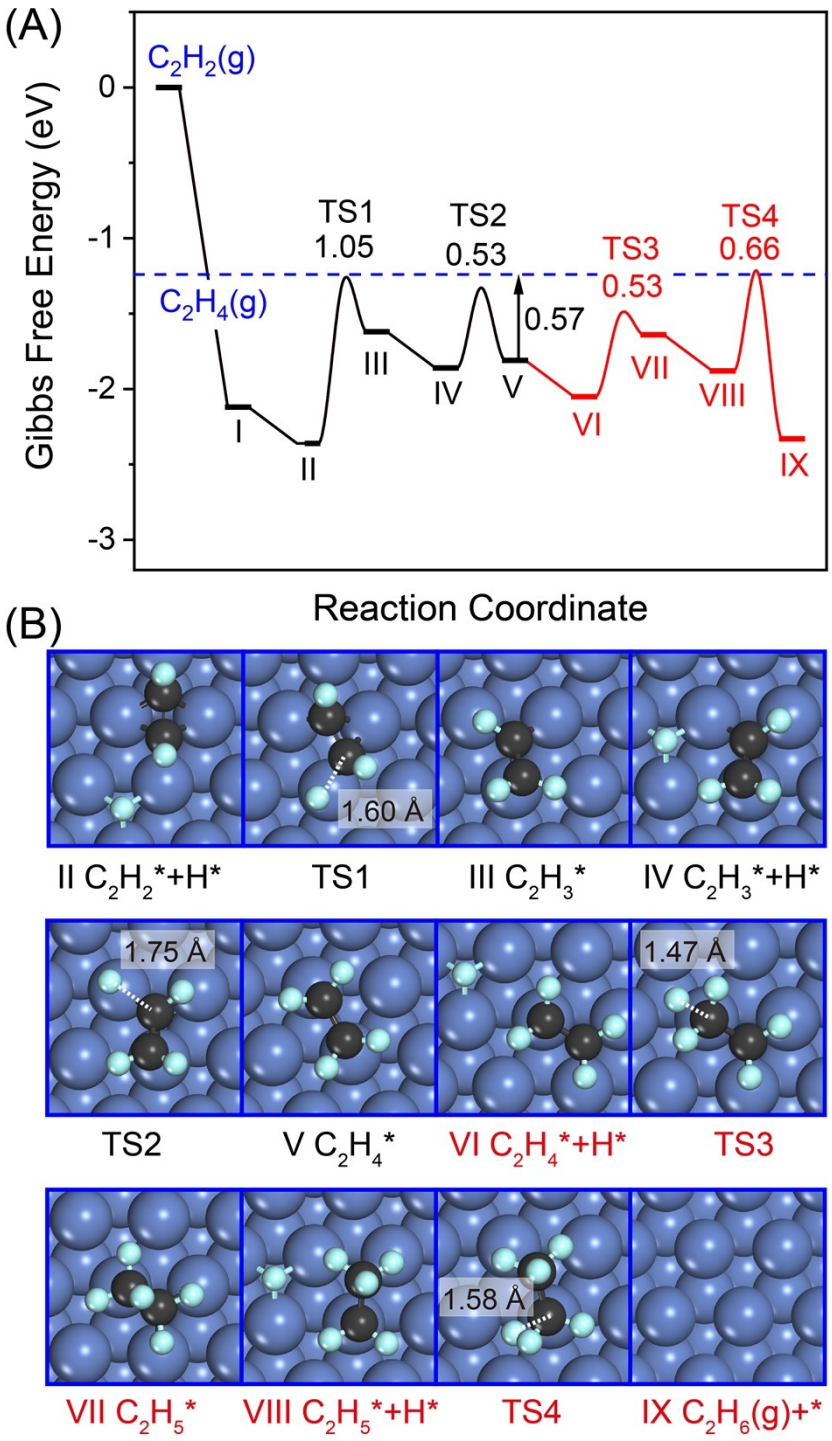


Figure S10. Gibbs free energy diagram for acetylene hydrogenation towards ethane on over Ni (111) with energy reference of acetylene and hydrogen molecule in gas phase. The blue dashed line represents the ethylene in gas phase. Corresponding structures of sequential hydrogenation of acetylene to ethylene and to ethane over Ni (111) were listed in below. Blue, black and green balls are nickel, carbon and hydrogen atoms, respectively. Reaction condition: T=360K, P=0.1MPa with 0.5% $C_2H_2$, 25% $C_2H_4$ and 5% $H_2$.

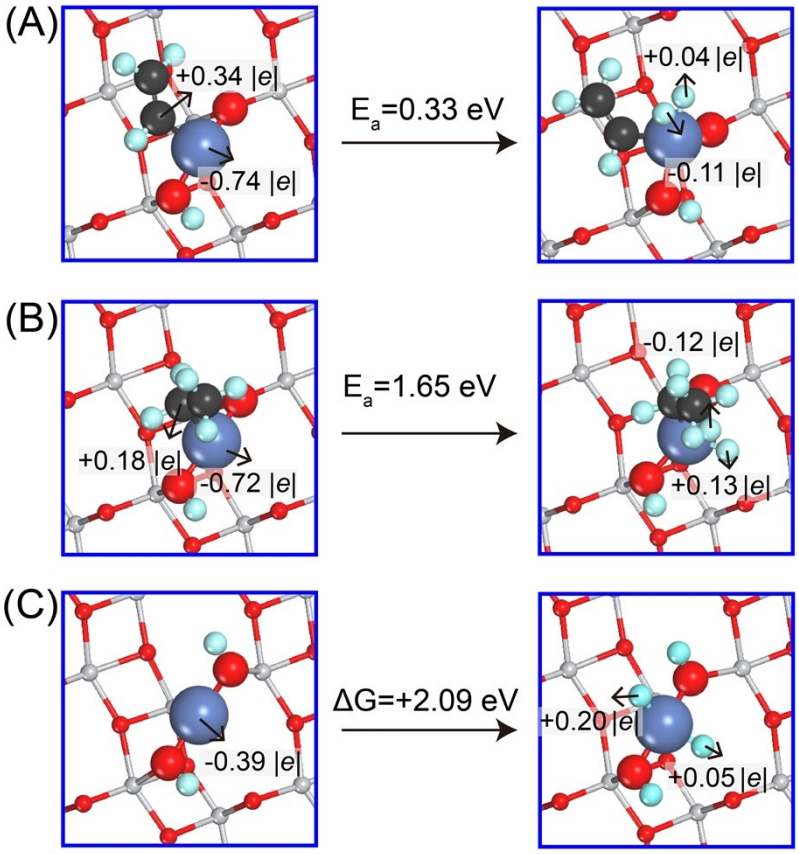


Figure S11. Top view of the dissociation of $H_2$ on $C_2H_3$-ligand (A), $C_2H_5$-ligand (B) and pristine $Ni_1(OH)_2/TiO_2$ (C). The activation energy ($E_a$) with Gibbs free energy correction and reaction Gibbs free energy ($\Delta G$) are reported therebetween the structures. The Bader charge is reported near the atom in the structure. Reaction condition: T=360K, P=0.1MPa with 0.5% $C_2H_2$, 25% $C_2H_4$ and 5% $H_2$.

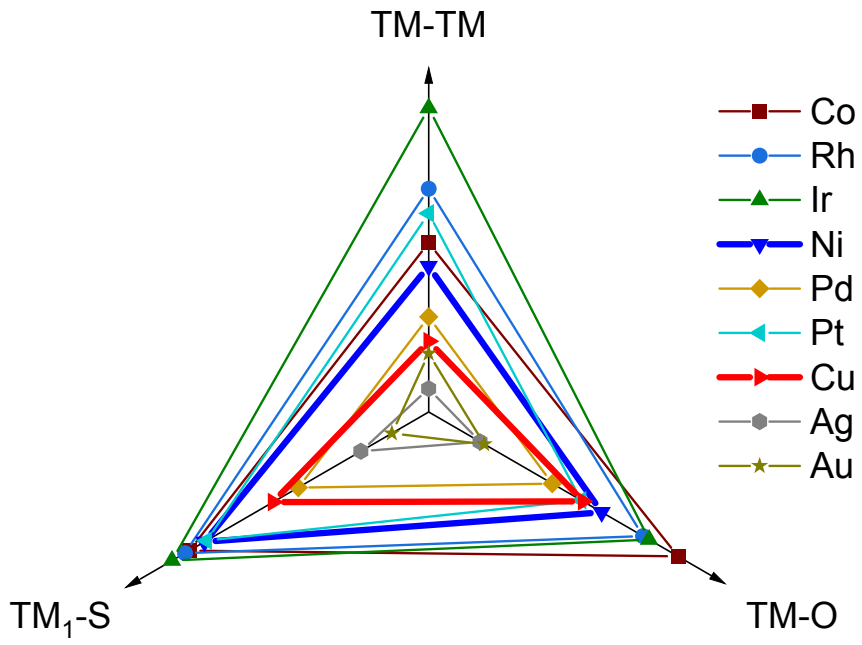


Figure S12. The radar plot for three kind of bond interaction. TM-TM, TM-O and $TM_1$-S are represented by metal cohesive energy, formation energy of traditional metal oxides and binding energy of $TM_1$ on metal oxides respectively. The stronger the interaction along the axis and the corresponding date is listed in Table S3.

Table S1. Calculated acetylene and ethylene adsorption energies without ZPE ($E_{ads}$, in eV), adsorption Gibbs free energy ($G_{ads}$, in eV) at 360 K under 0.1Mpa (0.5% $C_2H_2$, 25% $C_2H_4$ and 5% $H_2$, respectively) as well as geometries (distance in Å) for the various site on Ni (111) surface.

| | Site | $E_{ads}$ | $G_{ads}$ | C-M distance | C-C distance | C-H distance | C-C-H angle | torsion |
|---|---|---|---|---|---|---|---|---|
| $C_2H_2$ | π | -1.33 | -0.54 | 1.91 | 1.31 | 1.09 | 139.25° | |
| | di-σ | -1.83 | -1.03 | 1.85 | 1.34 | 1.10 | 128.29° | |
| | parallel-bridge | -2.60 | -1.78 | 1.94 | 1.39 | 1.10 | 125.45° | |
| | μ-bridge | -2.94 | -2.12 | 1.99 | 1.40 | 1.10 | 122.36° | |
| $C_2H_4$ | π | -1.16 | -0.46 | 2.03 | 1.42 | 1.10 | | 148.88° |
| | di-σ | -1.07 | -0.44 | 2.01 | 1.45 | 1.10 | | 139.84° |
| | Parallel-bridge | -1.13 | -0.48 | 2.12 | 1.45 | 1.12 | | 136.60° |
| | Perpendicular-bridge | -1.20 | -0.57 | 2.12 | 1.44 | 1.11 | | 139.80° |

Table S2. Calculated acetylene and ethylene adsorption energies without ZPE ($E_{ads}$, in eV), adsorption Gibbs free energy ($G_{ads}$, in eV) at 360 K under 0.1Mpa (0.5% $C_2H_2$, 25% $C_2H_4$ and 5% $H_2$, respectively) as well as geometries (distance in Å) for various $Ni_1$ catalysts.

| | $Ni_1/TiO_2$ | | $Ni_1(OH)\_H/TiO_2$ | | $Ni_1(OH)_2/TiO_2$ | |
|---|---|---|---|---|---|---|
| | $C_2H_2$ | $C_2H_4$ | $C_2H_2$ | $C_2H_4$ | $C_2H_2$ | $C_2H_4$ |
| $E_{ads}$ | -1.16 | -1.39 | -1.37 | -1.15 | -1.44 | -0.79 |
| $G_{ads}$ | -0.43 | -0.68 | -0.59 | -0.43 | -0.69 | -0.13 |
| C-M-distance | 1.98 | 2.01 | 1.93 | 1.97 | 1.87 | 2.00 |
| C-C-distance | 1.25 | 1.40 | 1.27 | 1.42 | 1.29 | 1.39 |
| C-H-distance | 1.08 | 1.10 | 1.09 | 1.10 | 1.09 | 1.10 |
| C-C-H-angle | 159.24° | | 156.19° | | 149.43° | |
| torsion | | 159.64° | | 155.41° | | 161.23° |

Table S3. Energy integral (-ICOHP, in eV/bond) values (separate orbital channels) for adsorption of $C_2H_2$ /$C_2H_4$ on different $Ni_1$ catalysts.

| | 4s | $3d_{xy}$ | $3d_{yz}$ | $3d_{z2}$ | $3d_{xz}$ | $3d_{x2-y2}$ | Sum |
|---|---|---|---|---|---|---|---|
| $C_2H_2/Ni_1$ | 0.70 | 0.03 | 0.12 | 0.19 | 0.60 | 0.04 | 1.69 |
| $C_2H_2/Ni_1(OH)\_H$ | 0.66 | 0.09 | 0.04 | 0.13 | 0.36 | 0.68 | 1.96 |
| $C_2H_2/Ni_1(OH)_2$ | 0.79 | 0.10 | 0.10 | 0.15 | 0.26 | 0.84 | 2.25 |
| $C_2H_4/Ni_1$ | 0.67 | 0.02 | 0.10 | 0.26 | 0.51 | 0.02 | 1.59 |
| $C_2H_4/Ni_1OH\_H$ | 0.62 | 0.07 | 0.09 | 0.13 | 0.41 | 0.47 | 1.79 |
| $C_2H_4/Ni_1(OH)_2$ | 0.64 | 0.07 | 0.27 | 0.13 | 0.34 | 0.20 | 1.65 |

Table S4. The Bader charge of Ni, Ti, O and $C_xH_y$ intermediates over $Ni_1(OH)_2/TiO_2$ catalyst during the reaction cycle as well as Ni and O in $Ni_1/TiO_2$ catalyst.

| | Ni | Ti[a] | O[b] | $C_xH_y$[c] |
|---|---|---|---|---|
| β-$Ni(OH)_2$-bulk | +1.18 | | | |
| Clean $TiO_2$ | | +2.04 | -0.91 | |
| $Ni_1/TiO_2$ | +0.73 | | | |
| $Ni_1(OH)_2/TiO_2$ | +0.39 | +1.88 | -1.16 | |
| $Ni_1(OH)\_H/TiO_2$ | +0.71 | +2.00 | -1.08 | |
| $C_2H_2$ | +0.54 | +2.00 | -1.19 | -0.25 |
| $C_2H_2$-H | +0.73 | +2.01 | -1.10 | -0.05 |
| $C_2H_3$ | +0.74 | +2.00 | -1.09 | -0.05 |
| $C_2H_4$-H | +0.72 | +2.01 | -1.06 | -0.02 |
| $C_2H_4$ | +0.72 | +1.83 | -1.22 | -0.07 |
| $C_2H_5$ | +0.72 | +1.99 | -1.05 | +0.03 |

[a] The Bader charge of surface Ti atom underneath Ni atom.

[b] The averaged Bader charge of O coordinated with Ni atom.

[c] The Bader charge of hydrocarbon species, in which co-adsorbed H is not included.

Table S5. The interaction energy (in eV) among metals and metal oxides, including metal cohesive energy, the formation energy of traditional metal oxides, binding energy of $TM_1$ on metal oxides and the formation energy of metal oxide, which represents the interaction of $TM_1$-$TM_1$, $TM_1$-O, $TM_1$-Support and M-O, respectively.

| | Molar volume $\Omega$($cm^3$) | Overall surface energy $\gamma$($J/m^2$) | Cohesive Energy | Formation energy of TM oxides | Binding energy of $TM_1$ | | | |
|---|---|---|---|---|---|---|---|---|
| | | | | | $TiO_2$ | $ZrO_2$ | $NbO_2$ | $IrO_2$ |
| Co | 6.67 | 2.34 | 5.54 | -1.41[a] | -3.82 | | | |
| Rh | 8.28 | 2.12 | 6.51 | -1.24[a] | -3.88 | | | |
| Ir | 8.52 | 2.42 | 7.96 | -1.27[a] | -4.06 | | | |
| Ni | 6.59 | 2.04 | 5.12 | -1.04[a] | -3.61 | -3.36 | -3.76 | -4.67 |
| Pd | 8.56 | 1.43 | 4.21 | -0.80[a] | -2.31 | | | |
| Pt | 9.09 | 1.59 | 6.07 | -0.94[a] | -3.58 | | | |
| Cu | 7.11 | 1.39 | 3.77 | -0.95[a] | -2.66 | | | |
| Ag | 10.27 | 0.79 | 2.92 | -0.45[a] | -1.44 | | | |
| Au | 10.21 | 0.76 | 3.55 | -0.47[a] | -1.01 | | | |
| Formation of metal oxides | | | | | -3.51[a] | -3.81[a] | -2.87[a] | -1.01[a] |

[a] Data from Material Project.[1]

Table S6. Calculated adsorption energy (in eV) without ZPE of acetylene and ethylene on single atom site ($M_1$-site) and metal site in oxide support ($M_s$-site).

| | $C_2H_2$ | | $C_2H_4$ | |
|---|---|---|---|---|
| | $M_1$-site | $M_s$-site | $M_1$-site | $M_s$-site |
| $Ni_1(OH)_2/TiO_2$ | -1.44 | -0.76 | -0.79 | -0.74 |
| $Cu_1(OH)_2/TiO_2$ | -1.07 | | -1.19 | |
| $Ni_1(OH)_2/NbO_2$ | -1.45 | -1.54 | -0.69 | -0.88 |
| $Ni_1(OH)_2/IrO_2$ | | -1.62 | | -0.89 |

References

1 A. Jain and S. P. Ong, *APL Mater*, 2013, **1**, 011002.